Fluorescence and Kinetic Analysis of the SpoIIAB Phosphorylation Reaction, a Key Regulator of Sporulation in *Bacillus subtilis*†

Joanna Clarkson,‡ Jwu-Ching Shu,‡ David A. Harris,§ Iain D. Campbell,§ and Michael D. Yudkin*,‡

Microbiology Unit, Department of Biochemistry, University of Oxford, South Parks Road, Oxford OX1 3QU, and Department of Biochemistry, University of Oxford, South Parks Road, Oxford OX1 3QU, U.K.

Received November 11, 2003; Revised Manuscript Received January 20, 2004

ABSTRACT: Sporulation in *Bacillus subtilis* provides a valuable model system for studying differential gene expression. The anti-sigma factor SpoIIAB is a bifunctional protein, responsible for regulating the activity of the first sporulation-specific sigma factor, σ^F. SpoIIAB can either bind to (and thus inhibit) σ^F or phosphorylate the anti-anti-sigma factor SpoIIAA. The phosphorylation reaction follows an unusual time course in which a pre-steady-state phase is succeeded by a slower steady-state phase. Previous experiments have shown that in the steady-state phase SpoIIAB is unable to inhibit σ^F. A fluorescent derivative of SpoIIAB (AB-F97W) was made that was indistinguishable from the wild type in its interactions with SpoIIAA and σ^F. AB-F97W exhibited distinctive changes in its fluorescence intensity when bound to ATP, ADP, or SpoIIAA. By following changes in the fluorescence properties of AB-F97W during the phosphorylation reaction, we confirmed a previous hypothesis that during the steady-state phase the predominant species are SpoIIAA·SpoIIAB·ADP complexes. The formation of these complexes is responsible for the slowing of the reaction, an important feature during sporulation since it reduces the loss of ATP in the nutrient-deprived cell. We also show that, to form a complex with SpoIIAA and ADP during the reaction, SpoIIAB must undergo a change in state which increases its affinity for ADP, and that this change in state is stimulated by its interaction with SpoIIAA. We derive a model of the reaction using previously determined kinetic and binding constants, and relate these findings to the known structure of SpoIIAB.

One of the most tractable systems for the study of differential gene expression is sporulation, the synthesis of endospores in *Bacillus subtilis*, which is initiated when *Bacillus* cells are starved of certain nutrients. An early feature of sporulation is an asymmetric division of the cell into two compartments, a smaller prespore and a larger mother cell, which immediately embark on different programs of gene expression. The progress of sporulation depends on the successive activation of specific sigma factors (transcription factors) in the two compartments. These sigma factors direct RNA polymerase to transcribe genes that are appropriate both to the location (prespore or mother cell) and to the temporal stage that sporulation has reached. The first such sigma factor is σ^F, which becomes active in the prespore soon after asymmetric septation. σ^F is present in the cell before sporulation begins, but it is kept inactive until asymmetric septation occurs. If σ^F is activated at the right time and in the right compartment, then (barring any other problem) the remaining sigma factors will be correctly activated in their turn and sporulation will progress to completion. Thus, the accurate regulation of σ^F is crucial to the success of sporulation (for a review, see ref *1*).

Three proteins are involved in regulating σ^F: SpoIIAB (AB),[1] SpoIIAA (AA), and SpoIIE. AB has two functions. It can act either as an anti-sigma factor (that is, it can bind to and inhibit σ^F) or as a specific protein kinase to phosphorylate AA on residue serine 58. To carry out either of these functions, AB must have ATP in its nucleotide-binding site. Alternatively, in the presence of ADP, AB can form a relatively long-lived complex with AA. Before asymmetric septation, and in the mother cell after asymmetric septation, all the AA is phosphorylated. AA-P has a very low affinity for AB, and the latter is therefore left free to bind to σ^F and prevent it from acting as a transcription factor. But when asymmetric septation is completed, SpoIIE, a specific protein phosphatase that hydrolyzes AA-P to AA, is activated in the prespore. The resulting AA can then interact with the σ^F·AB·ATP complex to induce the release of σ^F, itself becoming phosphorylated to AA-P (*2*). Following its release, σ^F remains active in sporulating cells for at least 2 h after asymmetric division (*3*). To account for this sustained activity of σ^F in the prespore, we have suggested that AA is repeatedly cycled through its phosphorylated and nonphosphorylated forms by AB, its kinase, and SpoIIE, its phosphatase (*4*). This cycling sequesters the AB kinase over a long period of time, preventing it from inhibiting σ^F.

† This work was supported by the Biotechnology and Biological Sciences Research Council (U.K.).

* To whom correspondence should be addressed. E-mail: mdy@bioch.ox.ac.uk.

‡ Microbiology Unit, Department of Biochemistry.

§ Department of Biochemistry.

[1] Abbreviations: AB, SpoIIAB; AA, SpoIIAA; AA-P, SpoIIAA phosphate.

10.1021/bi036014+ CCC: $27.50
Published on Web 02/27/2004

The phosphorylation of AA catalyzed by AB in vitro follows a biphasic time course, with a moderate pre-steady-state rate being succeeded by a slow steady-state rate after one cycle of the phosphorylation reaction (*4*). Previous results from this laboratory (*4*−*7*) led to the suggestion that the reduction in rate may be due to the formation of complexes between AA and the AB·ADP complex formed by the phosphorylation reaction. If this hypothesis is correct, AA·AB·ADP complexes should accumulate during the second phase of the phosphorylation reaction.

We chose to monitor the different states of AB by fluorescence spectroscopy. In these experiments, we observed changes in the fluorescent properties of a single tryptophan residue, which we introduced by mutagenizing F97 of AB to tryptophan (wild-type AB contains no tryptophan residues). F97 lies within the "ATP lid" region of AB, as seen in a recently published crystallographic structure of AB (*8*). The mutant protein was shown to be indistinguishable from the wild type both in its kinetics as measured in vitro and in its activity in vivo. The fluorescence intensity of this protein was found to respond reproducibly and distinctively to the binding of ADP, ATP, and AA. In addition, the fluorescence anisotropy of AB-F97W was found to respond reproducibly to AA binding. By following these properties during phosphorylation reactions, we were able to distinguish changes in the predominant state of the AB and thus investigate the mechanism by which sporulation is regulated.

EXPERIMENTAL PROCEDURES

Production of SpoIIA Proteins. To produce the mutant protein AB-F97W, site-directed mutagenesis was carried out by the method of Ho et al. (*9*), with a pET plasmid containing the *spoIIAB* gene (*10*) as a template. The primers used to amplify the entire gene by PCR were AB-FW (5′-AAAA-AAACATATGAAAAATGAAATGCACCTTGAG-3′) and AB-BW (5′-AAAGGATCCTTAATTACAAAGCGCTTT-GCT-3′), where the FW primer introduces an *Nde*I site at the beginning of the gene and the BW primer introduces a *Bam*HI site at the end. The primers used for the site-directed mutagenesis were AB-F97W-FW (5′-GTCAGCCTCTATG-GACGACTAA-3′) and AB-F97W-BW (5′-GGCTTAGTC-GTCCATAGAGGC-3′). The mutated gene was digested with *Nde*I and *Bam*HI and ligated into plasmid pET11a for expression in *Escherichia coli*. Other plasmids used for production of SpoIIA proteins were described by Diederich et al. (*10*) and Lee et al. (*6*). Expression and purification of SpoIIA proteins were carried out as described by Lee et al. (*6*). All proteins were prepared in a buffer containing 50 mM Tris-HCl (pH 7.5), 50 mM KCl, 1 mM DTT, and 0.5 mM $MgCl_2$.

With the exception of the nucleotide binding experiments, AB-F97W was used at a concentration of 0.5 μM for all in vitro experiments. This concentration produced suitable levels of fluorescence intensity and a suitable rate of incorporation of labeled phosphate into AA. It is also similar to the concentrations that occur in vivo (*4*). To provide extra sensitivity and accuracy in the nucleotide binding experiments, AB-F97W was used at a concentration of 1 μM. AA proteins were used at a concentration of 2 μM for binding experiments, to saturate AB-F97W with a 2-fold excess in the protomer concentration. For phosphorylation reactions, an AA concentration of 5 μM was used, to mimic the recycling of AA by the phosphatase SpoIIE and provide a significant number of turnovers in the reaction. Since the mutant AA-L90A has a faster turnover rate than wild-type AA (*6*), the concentration used in the reactions was increased to 7 μM so that a stable steady-state phase could be observed.

Incorporation of Labeled Phosphate into AA. The kinetics of phosphorylation of AA by AB were determined by assessing the incorporation of radioactivity from the γ-phosphate of ATP into an acid-insoluble form over time. These experiments were carried out with the method described by Lee et al. (*6*), except that incubation was carried out at 25 °C. Since the results are expressed in terms of radioactivity counts in the precipitated protein, the exact values depend on the batch of [γ-^{32}P]ATP that is used.

Fluorescence Spectroscopy. A Perkin-Elmer LS50B luminescence spectrometer, fitted with a fast filter accessory, was used to perform these experiments, and the results were analyzed with Perkin-Elmer FL WinLab software. All experiments were performed at 25 °C.

Steady-state fluorescence measurements were carried out using an excitation wavelength of 290 nm, with a slit width of 7.5 nm. Initial emission spectra were collected over 5 min between wavelengths of 300 and 450 nm, with a slit width of 7.5 nm.

The maximum fluorescence emission of AB-F97W in buffer alone was found to be at 355 nm, and hence, this wavelength was used to measure changes in fluorescence emission intensities. Emitted fluorescence intensities were recorded every second. Changes in the fluorescence intensity were observed with the addition of nucleotide. The percentage reduction in intensity was based on an average value in the absence of nucleotide obtained over a time period of 30 s. To determine intensity values upon the addition of nucleotide, small aliquots (less than 1% of the total volume) of nucleotide were added, and measurements were started immediately. To determine values at equilibrium in the presence of nucleotide, small aliquots of nucleotide were added, and once it had become stable, the average fluorescence signal was calculated over a time period of 30 s. Control experiments in which the nucleotide was replaced with buffer showed that the changes in fluorescence observed were not due to dilution effects.

Fluorescence anisotropy measurements were acquired using an excitation wavelength of 290 nm with a slit width of 7.5 nm and an emission wavelength of 355 nm with a slit width of 10 nm. An acquisition time of 2 s was used for each data point. Anisotropy values were calculated with the Perkin-Elmer software. The change in anisotropy upon addition of nucleotide was calculated using an average value in the absence of nucleotide obtained over the course of 2 min.

The results shown in this paper are from single experiments. However, to determine the reproducibility of the data, all experiments were repeated several times. In all cases, similar results were obtained. While specific values of fluorescence intensity change were found to be highly reproducible for a given preparation of AB-F97W (errors of less than 2%), slight differences in fluorescence intensity changes were noted between different preparations. Therefore, where in this paper experiments are compared directly with each other (i.e., within each figure), all data were obtained with a single preparation of AB-F97W.

At the concentrations used in these experiments, the addition of nucleotide gave no significant fluorescence intensity in the absence of AB-F97W. Control experiments in which nucleotide was added to wild-type AB or AA showed no significant change in the faint fluorescence intensity of these proteins. Concentrations of nucleotide that were used were restricted to <200 μM to prevent the inner filter effect, which was found experimentally to become significant above 500 μM. This finding is in agreement with the theoretical reduction in fluorescence intensity, which at 500 μM is 3.5% (*11*). In most of the experiments, a nucleotide concentration of 100 μM was used. At this concentration, the theoretical inner filter effect is 0.7%, which is within the error of the measurements.

Replacement of Wild-Type AB in B. subtilis. The mutation that replaces F97 of AB with W was introduced into the sequence of the entire *spoIIA* locus by the site-directed mutagenesis method of Ho et al. (*9*). Genomic DNA from wild-type *B. subtilis* strain 168ED was used as a template. The primers used to amplify the entire *spoIIA* locus were FW-AA-B$_{SalI}$ (5′-GGTCGACACTCTTGTTCTGAAAAAG-3′) and BW-AC-R$_{BamHI}$ (5′-GTAGTATGTGGATCCATTTTGT-TCTC-3′), where the FW primer introduces a *Sal*I site and the BW primer introduces a *Bam*HI site. The primers used for the site-directed mutagenesis were those described above for the production of the AB-F97W protein. The resulting PCR fragment was digested with *Sal*I and *Bam*HI and ligated into pMLK83 (*6*). The entire *spoIIA* locus was deleted from *B. subtilis* strain 168ED, and a *lacZ* reporter gene, under the control of the *spoIIQ* promoter, was integrated into the chromosome (for methods, see ref *6*). The pMLK83 plasmid containing the AB-F97W mutation was transformed into this strain and integrated into the *amyE* locus by double crossover. This strain was induced to sporulate, and the β-galactosidase activity (*6*) was compared to that in a Spo$^+$ strain in which a *lacZ* reporter had been integrated into strain 168ED. The σ^F activity was seen to be unaffected by the chromosomal position of the *spoIIA* locus. Later stages of sporulation, however, may be affected by such a change (*12*).

RESULTS

The Activity of AB-F97W Is Indistinguishable from That of Wild-Type AB. We used site-directed mutagenesis of genomic DNA to change residue 97 of AB from phenylalanine to tryptophan (see Experimental Procedures). Replacement of *spoIIAB*$^+$ by the mutant gene led to mutant bacteria, which activated σ^F at the normal time and to the normal extent (results not shown).

In vitro, the AB-F97W mutant protein was found by native PAGE binding assays to have an affinity for the AA·ADP complex similar to that of the wild-type protein. The kinetics of the AB-F97W phosphorylation reaction are shown in Figure 1. As previously shown for wild-type AB (*4*, *7*), the time course of the reaction (as assessed by the incorporation of radioactivity from the γ-phosphate of ATP into an acid-insoluble form) consisted of a moderate pre-steady-state phase that gave way after some 2−4 min to a slow steady-state phase.

Fluorescence Properties of AB-F97W. In our fluorescence spectroscopy experiments, we first established how the fluorescence properties of AB-F97W change on ligand binding. Fluorescence spectra of AB-F97W showed a maximum emission at 355 nm. Upon addition of 100 μM ADP or ATP, this fluorescence was shifted by approximately 1 nm to slightly shorter wavelengths, and reduced in intensity by up to 7%. Upon addition of ADP and AA, the fluorescence was shifted to shorter wavelengths by approximately 4 nm and reduced in intensity by 32−38% (see below). Since the reductions in intensity were more substantial than the shifts in wavelength, intensity was followed exclusively in subsequent experiments. As a further measure of AA binding, we determined changes in the fluorescence anisotropy of AB-F97W. The binding of AA gave rise to an increase in anisotropy values (r) of approximately 0.05 (see below).

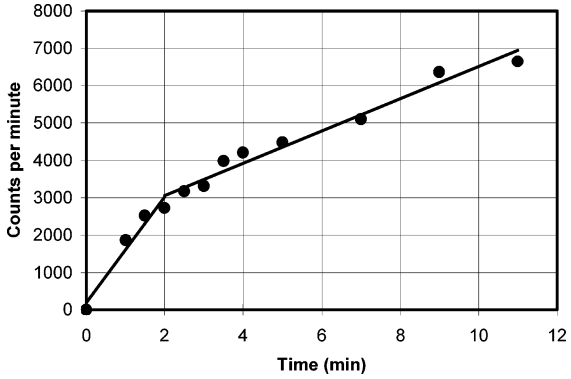

FIGURE 1: Kinetic behavior of AB-F97W (0.5 μM) in phosphorylating wild-type AA (5 μM), as measured by the extent of incorporation of ^{32}P from the γ-phosphate of ATP.

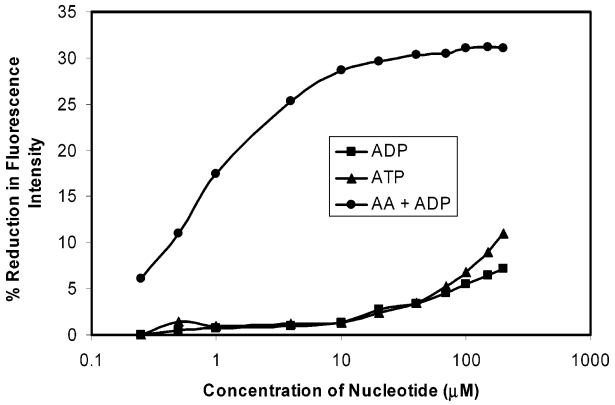

FIGURE 2: Effect of nucleotide on the fluorescence intensity of AB-F97W. AB-F97W was at a concentration of 0.5 μM, and where used, AA was at 2 μM. Values for the reduction in fluorescence intensity at equilibrium were calculated as described in Experimental Procedures. The effects of ADP (■), ATP (▲), and ADP in the presence of wild-type AA (●) are shown.

Figure 2 shows the reduction in fluorescence intensity of AB-F97W upon addition of varying concentrations of ADP or ATP. In the absence of AA, the addition of either ADP or ATP led to a change in fluorescence that increased with increasing nucleotide concentrations, but failed to reach a plateau even when nucleotide concentrations as high as 200 μM were added to 0.5 μM AB-F97W. (The nucleotide concentration was not increased above 200 μM as inner filter effects become significant at higher concentrations; see Experimental Procedures.) The addition of 100 μM ADP or ATP to 1 μM AB-F97W produced changes in fluorescence of different magnitudes, ATP giving the greater quenching. When AB-F97W was incubated with a mixture of ADP and

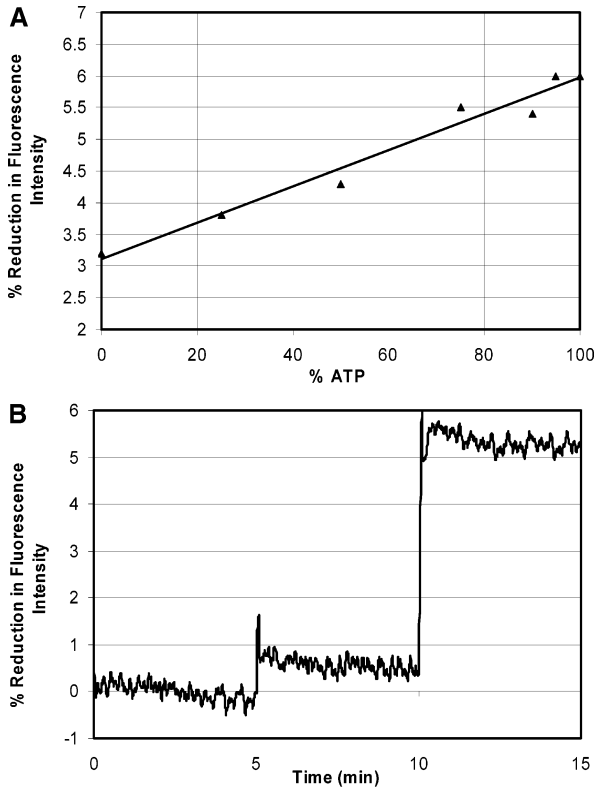

FIGURE 3: Effect of a mixture of nucleotides on the fluorescence intensity of AB-F97W. (A) Effect of varying ADP:ATP ratios. The total nucleotide concentration was 100 μM, and the concentration of AB-F97W was 1 μM. Values for the reduction in fluorescence intensity at equilibrium were calculated as described in Experimental Procedures. (B) Reductions in fluorescence intensity with time on the addition of nucleotide. The concentration of AB-F97W was 1 μM. ADP (25 μM) was added at 5 min and ATP (75 μM) at 10 min.

ATP (total concentration of 100 μM), the change in fluorescence was that expected from the ratio of their two concentrations (Figure 3A). Furthermore, when one of the nucleotides was added to a solution of AB-F97W that had previously been incubated with the other nucleotide, the fluorescence changed immediately, reaching an intensity of fluorescence that reflected the final ratio of the concentrations of the two nucleotides (Figure 3B). This shows that AB rapidly equilibrates with the surrounding nucleotide pool. This weak nucleotide binding and rapid nucleotide exchange are consistent with results obtained previously. Lord et al. (*13*) reported that the K_d for both AB·ADP and AB·ATP complexes is approximately 180 μM.

In the presence of AA, by contrast, the reduction in fluorescence approached a maximum at an ADP concentration as low as 10 μM (Figure 2). This result demonstrates that AB has an increased affinity for nucleotide in the presence of AA. (AA contains no tryptophan residue, and its intrinsic fluorescence does not interfere with that of AB-F97W.) Figure 4 shows the changes in fluorescence of AB-F97W over time on binding AA in the presence of 100 μM ADP (green line). There was a 34% decrease in fluorescence which was virtually complete within the mixing time. The rapid rate of AA binding shown in Figure 4 is consistent with kinetic constants obtained previously for this reaction (*4*). To see whether the intensity of fluorescence of an AA·AB-F97W·ATP complex could be distinguished from that of an

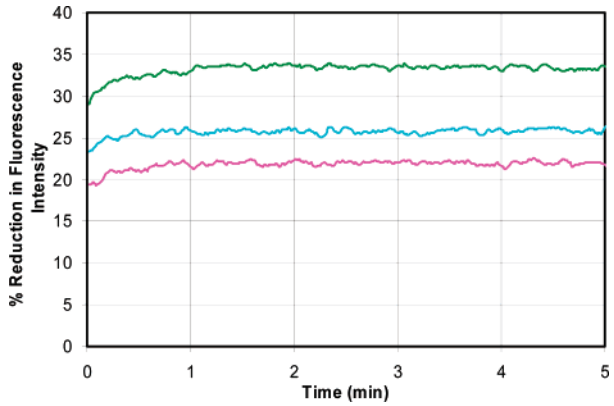

FIGURE 4: Effect of the formation of complexes with wild-type AA, AA-S58A, or AA-L90A on the fluorescence intensity of AB-F97W. AB-F97W was at a concentration of 0.5 μM; AA proteins were at a concentration of 2 μM and nucleotides at 100 μM. Reductions in the fluorescence intensity of AB-F97W with time are shown on binding to wild-type AA and ADP (green), AA-S58A and ADP (cyan), and AA-S58A and ATP (pink). Measurements were started on the addition of nucleotide to a mixture of the AA and AB proteins.

AA·AB-F97W·ADP complex, we used AA-S58A, a variant of AA that cannot be phosphorylated and hence forms a stable complex with ATP. As shown in Figure 4, the change in fluorescence was substantially different for the ADP and ATP complexes of S58A with AB-F97W, the ATP complex this time showing the smaller change (cyan and pink lines). The fact that the AB-F97W·ADP complex with AA-S58A (cyan line) has a fluorescence decrease smaller than that with wild-type AA (green line) is presumably due to the weaker affinity of the S58A mutant for the AB·ADP complex (*4*).

Time Course of Phosphorylation. Having established how the fluorescence properties of AB-F97W change on ligand binding, we were in a position to correlate temporal changes in these properties with the time course of the phosphorylation reaction, as measured by the incorporation of γ-phosphate from ATP into AA. We carried out three parallel phosphorylation reactions; in all of them, ATP (100 μM) was added to a mixture of AB-F97W (0.5 μM) and AA (5 μM). In the first experiment (blue line in Figure 5A) we measured changes in fluorescence intensity, in the second (Figure 5B) the incorporation of ^{32}P from γ-labeled ATP into AA, and in the third (blue line in Figure 5C) the change in fluorescence anisotropy on interaction of AB-F97W with AA. The blue line in Figure 5A shows that the fluorescence intensity of AB-F97W during the phosphorylation reaction diminished much more slowly than in the formation of the AA·AB-F97W·ADP complex (green line). A steady state was observed after only ~4 min. At the plateau, the reduction in fluorescence intensity approached that of the noncovalent ternary complex made between AB-F97W (0.5 μM), ADP (100 μM), and AA (5 μM) (green line in Figure 5A). When the steady-state phase ended, ~40 min from the beginning of the reaction, the fluorescence returned to the level that is characteristic of the binary complex between AB-F97W and ATP (see the red line in Figure 5A). These changes can be correlated with the time course of the reaction as measured by the incorporation of radioactivity (Figure 5B). Here, we can see that the approach to the steady-state level of fluorescence corresponds with the pre-steady-state rate of the reaction, that the plateau of reduced fluorescence

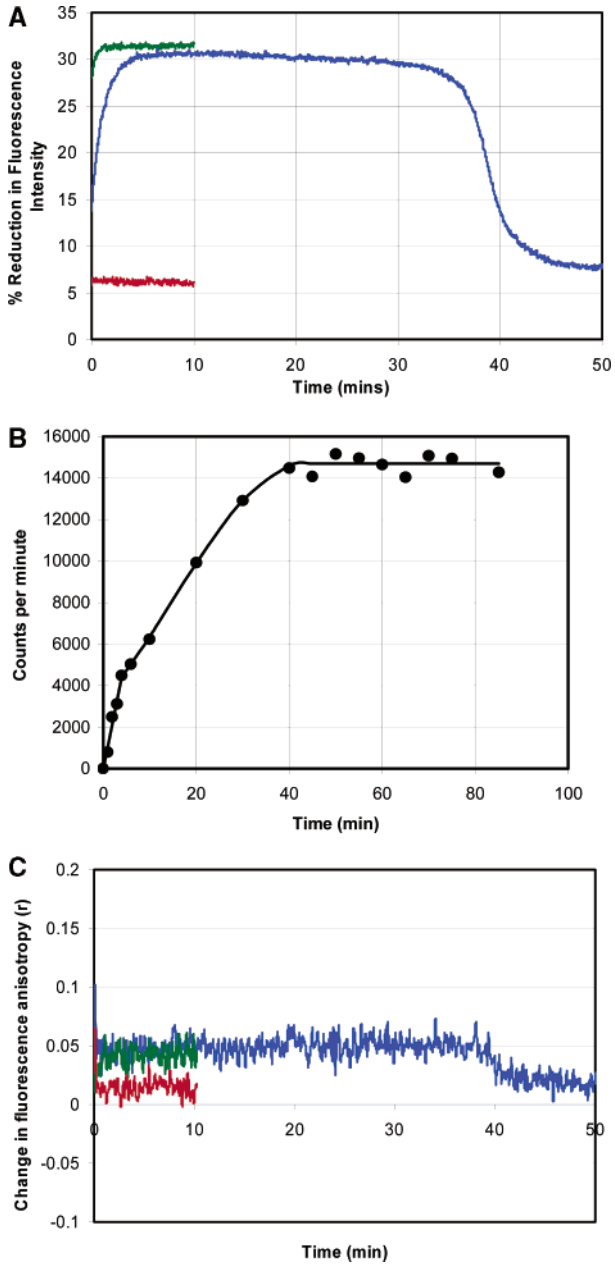

FIGURE 5: Parallel phosphorylation reactions of wild-type AA measuring (A, blue line) reductions in fluorescence intensity, (B) the incorporation of ^{32}P from γ-labeled ATP, and (C, blue line) the fluorescence anisotropy. The reaction mixtures contained AB-F97W (0.5 μM) and AA (5 μM), and the reactions were started on the addition of ATP (100 μM). (A and C) Red line: the addition of ATP (100 μM) to AB-F97W (0.5 μM) alone. Green line: the addition of ADP (100 μM) to a mixture of AB-F97W (0.5 μM) and AA (5 μM).

intensity corresponds with the steady-state rate of reaction, and that the end of the phosphorylation reaction corresponds to the time at which the fluorescence returns to a baseline value. Figure 5C shows the fluorescence anisotropy results, with the blue line representing the incubation containing ATP and the green line the formation of the ternary noncovalent complex. Here, by contrast, there is no pre-steady-state phase; in addition, the fluorescence anisotropy simply returns to its baseline value on completion of the phosphorylation reaction.

The anisotropy result (Figure 5C) demonstrates that AB-F97W is saturated with AA during the first few seconds of the phosphorylation reaction: there is no evidence for a gradual change in the molecular mass of the complex during the pre-steady-state phase. By contrast, the fluorescence intensity results reveal a gradual change in the state of AB-F97W during the pre-steady-state phase. We interpret the changes as follows. During the first few seconds, AA binds to the AB-F97W·ATP complex, and the fluorescence intensity of the resulting complex is reduced by ~20%. (Note that, as shown in Figure 4, formation of the AA·AB-F97W·ATP complex reduces the fluorescence intensity less than the formation of a AA·AB-F97W·ADP complex.) However, as the AB-F97W·ADP complex is formed in the reaction, most of it binds to AA, which is present in excess, to form a AA·AB-F97W·ADP complex. This results in a further reduction in fluorescence intensity to ~30%, which approaches the level characteristic of the AA·AB-F97W·ADP complex as the reaction reaches the steady state. At the same time, the formation of these complexes slows the overall rate of the reaction so that the steady-state rate is slower than the pre-steady-state rate (Figure 5B). When AA is exhausted (the reaction is completed), only AB-F97W·ATP complexes can form (see the end of the blue curve in Figure 5A).

A Mutant of AA that Cannot Form AA·AB·ADP Complexes. If the above interpretation of the changes in state of AB during the phosphorylation reaction is correct, then a different pattern of changes in fluorescence intensity would be expected if the reaction were repeated with a mutant of AA that has a much lower affinity for the AB·ADP complex. AA-L90A has a dissociation constant for the ternary complex (AA·AB·ADP) at least 100 times higher that of the wild type (*6*). Experiments were performed in which ATP (100 μM) was added to a mixture of AB-F97W (0.5 μM) and AA-L90A (7 μM). Figure 6A shows that the phosphorylation of AA-L90A proceeded much more rapidly, with linear kinetics, indicating that the slow step in the steady state of the wild-type reaction is faster in this mutant. The changes in fluorescence intensity during the phosphorylation of AA-L90A were strikingly different from those obtained with wild-type AA. Instead of gradually approaching a stable level over the course of several minutes, the fluorescence intensity quickly reached a steady state, and it remained in this steady state for ~10 min; thereafter, the fluorescence returned to the level characteristic of a binary AB-F97W·ATP complex (Figure 6B). The reductions in fluorescence intensity were substantially smaller than with wild-type AA.

Interactions with AA Produce a Change in the State of AB. The results described above lend support to the view that AA·AB-F97W·ADP complexes are formed after the first round of the phosphorylation reaction, and that the formation of such complexes is responsible for the diminution in rate of the steady-state phase (*5*). To establish this model more securely, we must consider how such ternary complexes can be produced, given an apparent discrepancy between the rate of association of AA with the AB·ADP complex and the rate of dissociation of that complex. Previously, Lord et al. (*13*) showed that AB has a relatively weak affinity for ADP ($K_d \approx 180$ μM). If it is assumed that the k_{on} for this interaction is in the range found for other associations between proteins and small ligands (*14*, *15*), this gives a k_{off} of approximately 10^3 s^{-1}. This relatively weak affinity of AB for ADP and fast nucleotide exchange were confirmed in the fluorescence results (Figures 2 and 3). It is therefore difficult to see how the AA·AB·ADP complex

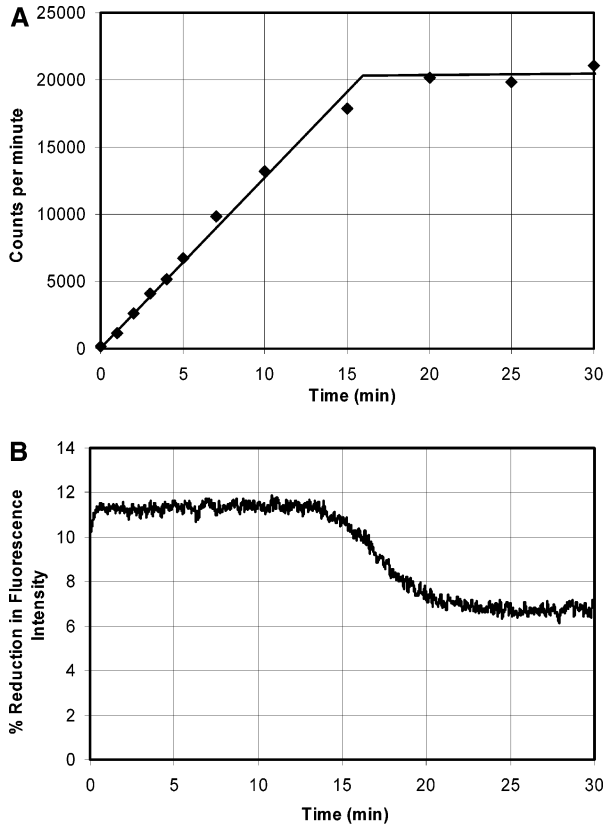

FIGURE 6: Parallel phosphorylation reactions of AA-L90A measuring (A) the incorporation of ^{32}P from γ-labeled ATP and (B) reductions in fluorescence intensity. The reaction mixtures contained AB-F97W (0.5 μM) and AA-L90A (5 μM), and the reactions were started on the addition of ATP (100 μM).

could accumulate, since the rate of association of AA with the AB·ADP complex [approximately 1.5 s^{-1} at 5 μM AA (*4*)] is much slower than the rate of dissociation of ADP from AB.

To investigate this point further, we carried out the following experiments. AA (5 μM) and AB (0.5 μM) were incubated together, and the reaction was started by adding ATP (100 μM) that had previously been mixed with 5 μM ADP. The observed reductions in the fluorescence intensity over time were identical to those in the absence of ADP (orange and blue lines in Figure 7A). Assessment of the incorporation of radioactive phosphate into AA (● and △ in Figure 7B) again showed that the rates of phosphorylation in the presence and absence of ADP were indistinguishable. Thus, the addition of ADP alone does not induce the slow step of the steady-state phase.

It appears therefore that to form AA·AB·ADP complexes, AB must undergo some change during the first round of the phosphorylation reaction that decreases the rate at which ADP dissociates from it. Since this change occurs during its interaction with AA, we tried to mimic this by preforming AA·AB·ADP complexes. AA (5 μM) was preincubated together with AB-F97W (0.5 μM) and 5 μM ADP for several minutes to allow AA·AB·ADP complexes to form. When ATP (100 μM) was subsequently added, it was clear that the pre-steady-state phase had been completely eliminated (black line in Figure 7A and ▲ in Figure 7B). Interaction with AA thus appears to produce a change in AB which decreases the rate at which ADP dissociates from it.

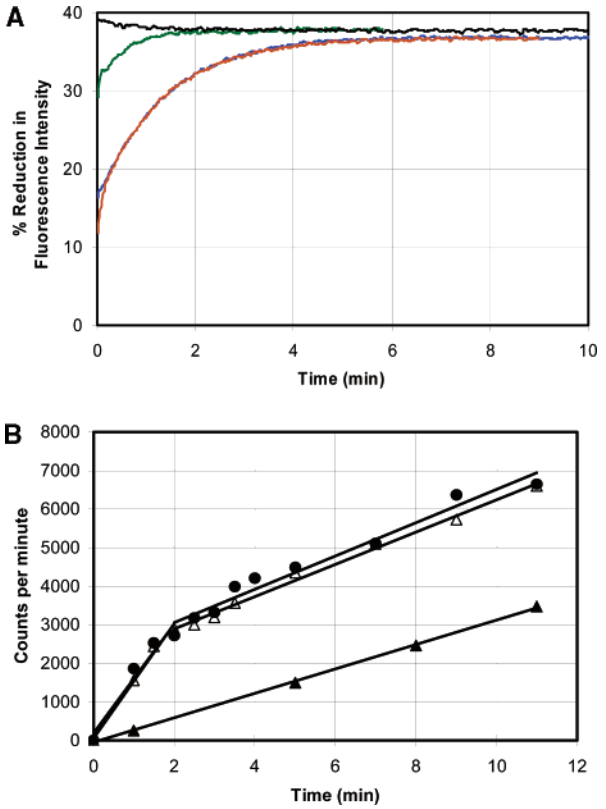

FIGURE 7: Parallel phosphorylation reactions of wild-type AA with added ADP. (A) Reductions in fluorescence intensity. (B) Uptake of ^{32}P from γ-labeled ATP. AB-F97W (0.5 μM) was mixed with AA (5 μM), and the reactions were started on the addition of nucleotide. Nucleotides that were added were 100 μM ATP (A, bright blue line; B, ●), 100 μM ADP (A only, green line), a mixture of 100 μM ATP and 5 μM ADP (A, orange line; B, △). Also shown are the changes that occurred when a mixture of SpoIIAB and SpoIIAA was preincubated with 5 μM ADP for 5 min and 100 μM ATP was added (A, black line; B, ▲).

DISCUSSION

The results presented here confirm the hypothesis that, during the steady-state phosphorylation of AA, AB exists predominantly in AA·AB·ADP complexes. Our results also show that to form such complexes AB must adopt a refractory conformation from which ADP dissociation is very slow. Figure 8A summarizes these findings in a phosphorylation scheme. In this scheme, we denote the change in the state of AB, occurring when it interacts with AA, with the superscript closed (the reason for this nomenclature is explained below).

In previous work, we have measured kinetic and binding constants for many of the steps shown in Figure 8A (*4*, *7*, *13*). It is attractive to attempt to analyze our current results and these previously determined constants in terms of the scheme shown in Figure 8A. To carry out this analysis, we use a simplified scheme as shown in Figure 8B, in which AB′ denotes the sum of species **1**−**4** and **6** in Figure 8A. In previous studies, the pre-steady-state rate constant and the steady-state rate constant have been determined. In our scheme in Figure 8A, the pre-steady-state rate constant will be equal to the rate constant for the reactions from the free AB to the formation of the first molecule of AA-P (reactions involving species **1**−**4**). Since we know that the rate of ADP−ATP exchange is very rapid (approximately 10^3 s^{-1}), we can assume that the rate constant k_i is equal to the pre-

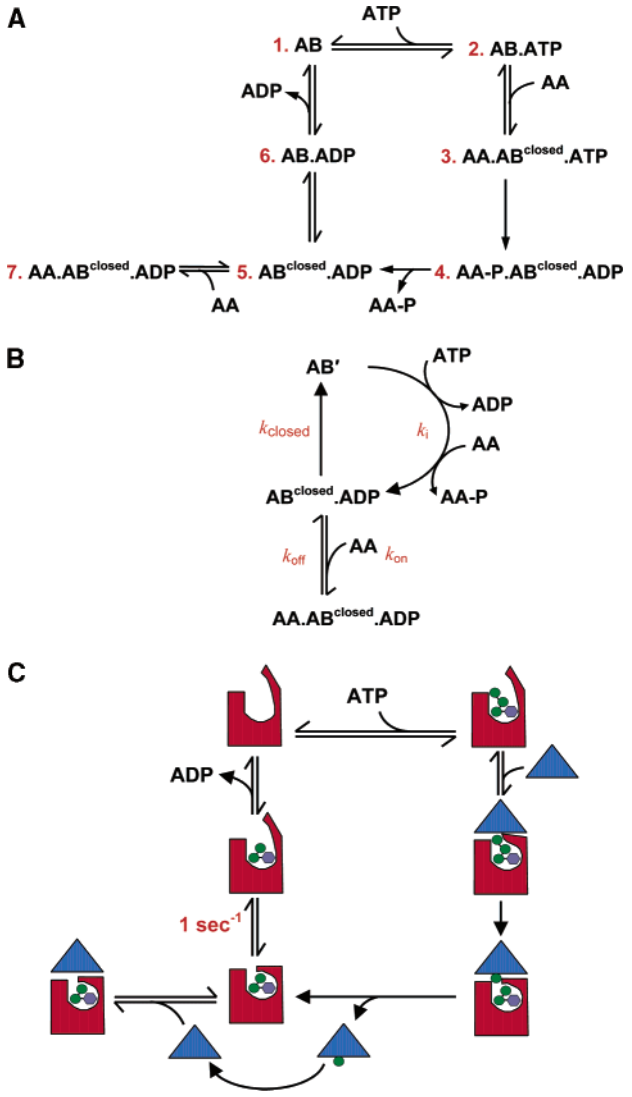

FIGURE 8: Proposed schemes for the phosphorylation of AA by AB. (A) Proposed phosphorylation pathway. During its interaction with AA, AB undergoes a change in state to the AB^{closed} form. This change decreases the rate at which ADP dissociates from AB, allowing the AA·AB^{closed}·ADP ternary complex to form. (B) A simplified pathway. (C) Mechanism for the pathway shown in terms of proposed conformational changes in AB. It is proposed that in the AB^{closed} form the ATP lid loop undergoes a conformational change such that nucleotide is trapped in the binding pocket: blue shape, SpoIIAA; red shape, SpoIIAB; purple hexagon, adenosine moiety of ADP and ATP; green circles, phosphate groups.

steady-state rate constant, which is approximately 5×10^{-3} s^{-1} (*4*, *7*). The rate-limiting step of this sequence is the phosphorylation reaction (conversion of species **3** to **4** in Figure 8A) (*7*). The rate constant k_{closed} for the AB^{closed}·ADP to AB reaction will be equal to the rate constant in the scheme in Figure 8A for the AB^{closed}·ADP to AB·ADP reaction. We can assume that this reaction is essentially irreversible as it is not possible to make the AB^{closed}·ADP complex by mixing AB and ADP. In the steady state, we can make the following assumptions:

$$k_{off}[AA{\cdot}AB^{closed}{\cdot}ADP] = k_{on}[AB^{closed}{\cdot}ADP][AA]$$

(equilibrium between $[AB^{closed}{\cdot}ADP]$ and $[AA{\cdot}AB^{closed}{\cdot}ADP]$) (1)

and

$$k_{closed}[AB^{closed}{\cdot}ADP] = k_i[AB'] = k_{cat}[AB^{total}] \quad (2)$$

(since this reaction is in steady state, the rate at which each intermediate is produced is equal to the rate of its breakdown. The rate at which AA is phosphorylated is equal to the rate at which AB′ is converted to the AB^{closed}·ADP complex) where

$$[AB^{total}] = [AB'] + [AB^{closed}{\cdot}ADP] + [AA{\cdot}AB^{closed}{\cdot}ADP] \text{ (conservation of mass)} \quad (3)$$

and k_{cat} is equal to the steady-state rate constant for the reaction, which is 0.8×10^{-3} s^{-1} (*4*, *7*).

To derive values for the relative quantities of the three components (AB′, AB^{closed}·ADP, and AA·AB·ADP) and therefore assess whether this model fits the fluorescence results, we must first derive the rate constant, k_{closed}. We derive k_{closed} as follows:

$$[AB'] = \frac{k_{closed}[AB^{closed}{\cdot}ADP]}{k_i} \text{ (from eq 2)}$$

$$[AA{\cdot}AB^{closed}{\cdot}ADP] = \frac{k_{on}[AB^{closed}{\cdot}ADP][AA]}{k_{off}} \text{ (from eq 1)}$$

$$k_{closed}[AB^{closed}{\cdot}ADP] = k_{cat}([AB'] + [AB^{closed}{\cdot}ADP] + [AA{\cdot}AB^{closed}{\cdot}ADP]) \text{ (from eqs 2 and 3)}$$

Expressing [AB′] and $[AA{\cdot}AB^{closed}{\cdot}ADP]$ in terms of $[AB^{closed}{\cdot}ADP]$

$$k_{closed}[AB^{closed}{\cdot}ADP] = k_{cat}\left(\frac{k_{closed}[AB^{closed}{\cdot}ADP]}{k_i} + [AB^{closed}{\cdot}ADP] + \frac{k_{on}[AB^{closed}{\cdot}ADP][AA]}{k_{off}}\right)$$

Dividing through

$$k_{closed} = k_{cat}\left(\frac{k_{closed}}{k_i} + 1 + \frac{k_{on}[AA]}{k_{off}}\right)$$

$$k_{closed}\left(1 - \frac{k_{cat}}{k_i}\right) = k_{cat}\left(1 + \frac{k_{on}[AA]}{k_{off}}\right)$$

Since the K_d for the dissociation of the AA·AB^{closed}·ADP complex equals k_{off}/k_{on}

$$k_{closed} = \frac{k_{cat}\left(1 + \frac{1}{K_d}[AA]\right)}{1 - \frac{k_{cat}}{k_i}}$$

Using a K_d value of 40 nM (*4*), k_i and k_{cat} taken from pre-steady-state and steady-state values of phosphorylation (see above) and a concentration of AA of 40 μM [the concentration of AA at which the kinetic constants were determined (*4*, *7*)], we find a k_{closed} value of 0.95 s^{-1}.

From the above equations, we can now estimate the proportions of the various components in the reaction in terms of the percentage that they represent of the total concentration of AB.

Fraction of AB^{closed}·ADP:

$$([AB^{closed}\cdot ADP]/[AB^{total}]) = \frac{k_{cat}}{k_{closed}} = 0.084\%$$

Fraction of AA·AB^{closed}·ADP:

$$([AA\cdot AB^{closed}\cdot ADP]/[AB^{total}]) = \frac{1}{K_d}[AA]\frac{[AB^{closed}\cdot ADP]}{[AB^{total}]} = 84\%$$

Fraction of AB′:

$$([AB']/[AB^{total}]) = \frac{k_{cat}}{k_i} = 16\% \text{ or}$$

$$([AB']/[AB^{total}]) = \frac{k_{closed}}{k_i}\frac{[AB^{closed}\cdot ADP]}{[AB^{total}]} = 16\%$$

If this model is correct, the relative concentrations of the AB^{closed}·ADP and AA·AB^{closed}·ADP complexes derived above should fit the K_d value for the formation of the ternary complex. From the definition of the K_d

$$K_d = \frac{[AA][AB^{closed}\cdot ADP]}{[AA\cdot AB^{closed}\cdot ADP]}$$

and using a total AB concentration of 0.5 μM and a AA concentration of 40 μM, a K_d value of 40 nM is obtained, which is consistent with our original value.

In the above analysis, the predominant species is the AA·AB^{closed}·ADP complex, a finding which is in accordance with the fluorescence results (see Figure 5A). Almost all of the remainder is in the AB′ form. AB′ will consist largely of the AA·AB·ATP complex, since it is known that the exchange of nucleotide and binding of AA are relatively rapid processes compared to the transfer of phosphate (*4*, *7*, *13*). From Figures 4 and 5A, we can estimate the relative fluorescence of an ATP-containing AA·AB complex compared to that of an ADP complex, by comparing the S58A·F97W·ATP complex with the wild-type AA·F97W·ADP complex and taking the value for the reduction in fluorescence after 1 min of the phosphorylation reaction, at which time the AB should be fully saturated with AA. [It is not possible to compare directly the two S58A complexes since it is known that the S58A mutation reduces the affinity of AA, particularly for the ADP-containing complex (*4*).] By comparing these two results, we estimate that the AA·AB·ATP complex has approximately 75% of the reduction in fluorescence of the AA·AB·ADP form. Therefore, a mixture of 84% AA·AB·ADP complexes and 16% AA·AB·ATP complexes would be expected to have a reduction in fluorescence of approximately 96% of the reduction due to the AA·AB·ADP complex alone. It is found from Figure 5A that during the steady-state phosphorylation reaction the reduction in fluorescence is 96.5% of that of the AA·AB·ADP complex. Therefore, it appears that our model, which was derived from the kinetic data previously published (*4*, *7*), fits well with the fluorescence results shown in Figures 4 and 5.

The crystal structure of AB, which was determined to 2.9 Å resolution (*8*), gives us an insight into how the change in state from AB to the AB^{closed} form may occur. AB adopts the GHKL superfamily fold. This superfamily includes bacterial histidine kinases, ATPases, and mitochondrial protein kinases (*16*−*18*). A common feature of this superfamily is a novel nucleotide binding fold, which includes a flexible loop known as the ATP lid. In many structures, such as AB, this loop covers the nucleotide-binding pocket. In some cases, an important feature for the biological activity of these proteins is the ability of their ATP lid to alter its conformation on binding ligands (*17*, *19*). This leads us to propose a mechanism to explain the change in state observed in AB (see Figure 8C). We propose that AB alone has an open, or disordered, ATP lid in which the nucleotide is relatively free to dissociate from the protein. However, on binding AA, the ATP lid adopts a closed conformation in which the nucleotide is more tightly bound. In the phosphorylation scheme, after the dissociation of AA-P this conformation persists briefly, relaxing back to the open conformation at a rate of $\sim$1 s^{-1}. It is this relatively slow rate of relaxation that maintains the AB·ADP complex for a sufficient amount of time to allow the AA·AB·ADP complex to form.

In the calculations presented above, we assumed that the AB^{closed}·ADP to AB·ADP reaction was essentially irreversible. However, from the thermodynamics AB must be able to adopt the closed conformation in the absence of AA, albeit forming that conformation at a very slow rate such that the equilibrium is far in favor of the open conformation. The binding of AA shifts that equilibrium in favor of the closed conformation. This point underlines the central importance of the concentration of dephosphorylated AA in the activation of σ^F. Dephosphorylated AA acts not only as a substrate that changes the conformation of AB but also as a ligand that forms a complex with this altered conformation. AA·AB·ADP complexes formed in this manner have been shown previously to be unable to interact with σ^F (*6*) so that their formation activates the transcription factor.

ACKNOWLEDGMENT

We thank H. Prescott for outstanding technical assistance and R. Lewis for valuable discussions.

REFERENCES

1. Kroos, L., Zhang, B., Ichikawa, H., and Yu, Y. T. (1999) Control of sigma factor activity during *Bacillus subtilis* sporulation, *Mol. Microbiol. 31*, 1285−1294.
2. Duncan, L., Alper, S., and Losick, R. (1996) SpoIIAA governs the release of the cell-type specific transcription factor σ^F from its anti-sigma factor SpoIIAB, *J. Mol. Biol. 260*, 147−164.
3. Partridge, S. R., and Errington, J. (1993) The importance of morphological events and intercellular interactions in the regulation of prespore-specific gene expression during sporulation in *Bacillus subtilis*, *Mol. Microbiol. 8*, 945−955.
4. Magnin, T., Lord, M., and Yudkin, M. D. (1997) Contribution of partner switching and SpoIIAA cycling to regulation of σ^F activity in sporulating *Bacillus subtilis*, *J. Bacteriol. 179*, 3922−3927.
5. Lee, C. S., Lucet, I., and Yudkin, M. D. (2000) Fate of the SpoIIAB*-ADP liberated after SpoIIAB phosphorylates SpoIIAA of *Bacillus subtilis*, *J. Bacteriol. 182*, 6250−6253.

6. Lee, C. S., Clarkson, J., Shu, J. C., Campbell, I. D., and Yudkin, M. D. (2001) *Bacillus subtilis* mutations that alter the pathway of phosphorylation of the anti-anti-σ^F factor SpoIIAA lead to a Spo- phenotype, *Mol. Microbiol. 40*, 9−19.
7. Najafi, S. M., Harris, D. A., and Yudkin, M. D. (1997) Properties of the phosphorylation reaction catalyzed by SpoIIAB that help to regulate sporulation of *Bacillus subtilis*, *J. Bacteriol. 179*, 5628−5631.
8. Campbell, E. A., Masuda, S., Sun, J. L., Muzzin, O., Olson, C. A., Wang, S., and Darst, S. A. (2002) Crystal structure of the *Bacillus stearothermophilus* anti-sigma factor SpoIIAB with the sporulation sigma factor σ^F, *Cell 108*, 795−807.
9. Ho, S. N., Hunt, H. D., Horton, R. M., Pullen, J. K., and Pease, L. R. (1989) Site-directed mutagenesis by overlap extension using the polymerase chain reaction, *Gene 77*, 51−59.
10. Diederich, B., Wilkinson, J. F., Magnin, T., Najafi, M., Errington, J., and Yudkin, M. D. (1994) Role of interactions between SpoIIAA and SpoIIAB in regulating cell-specific transcription factor σ^F of *Bacillus subtilis*, *Genes Dev. 8*, 2653−2663.
11. Kubista, M., Sjoback, R., Eriksson, S., and Albinsson, B. (1994) Experimental correction for the inner-filter effect in fluorescence spectra, *Analyst 119*, 417−419.
12. Dworkin, J., and Losick, R. (2001) Differential gene expression governed by chromosomal spatial asymmetry, *Cell 107*, 339−346.
13. Lord, M., Magnin, T., and Yudkin, M. D. (1996) Protein conformational change and nucleotide binding involved in regulation of σ^F in *Bacillus subtilis*, *J. Bacteriol. 178*, 6730−6735.
14. Bagshaw, C. R., and Trentham, D. R. (1974) The characterization of myosin-product complexes and of product-release steps during the magnesium ion-dependent adenosine triphosphatase reaction, *Biochem. J. 141*, 331−349.
15. Fersht, A. (1999) *Structure and mechanism in protein science*, Freeman, New York.
16. Dutta, R., and Inouye, M. (2000) GHKL, an emergent ATPase/kinase superfamily, *Trends Biochem. Sci. 25*, 24−28.
17. Machius, M., Chuang, J. L., Wynn, R. M., Tomchick, D. R., and Chuang, D. T. (2001) Structure of rat BCKD kinase: nucleotide-induced domain communication in a mitochondrial protein kinase, *Proc. Natl. Acad. Sci. U.S.A. 98*, 11218−11223.
18. Steussy, C. N., Popov, K. M., Bowker-Kinley, M. M., Sloan, R. B., Jr., Harris, R. A., and Hamilton, J. A. (2001) Structure of pyruvate dehydrogenase kinase. Novel folding pattern for a serine protein kinase, *J. Biol. Chem. 276*, 37443−37450.
19. Bilwes, A. M., Quezada, C. M., Croal, L. R., Crane, B. R., and Simon, M. I. (2001) Nucleotide binding by the histidine kinase CheA, *Nat. Struct. Biol. 8*, 353−360.

BI036014+